Biophysical Chemistry 159 (2011) 205–209

Contents lists available at ScienceDirect

Biophysical Chemistry

journal homepage: http://www.elsevier.com/locate/biophyschem

Linkage of cation binding and folding in human telomeric quadruplex DNA

Robert D. Gray, Jonathan B. Chaires *

James Graham Brown Cancer Center, 505 S. Hancock St., University of Louisville, Louisville, KY 40202, United States

ARTICLE INFO

Article history:
Received 9 June 2011
Received in revised form 20 June 2011
Accepted 20 June 2011
Available online 28 June 2011

Keywords:
Human telomere
G-quadruplex
Potassium binding
Folding-cation linkage

ABSTRACT

Formation of DNA quadruplexes requires monovalent cation binding. To characterize the cation binding stoichiometry and linkage between binding and folding, we carried out KCl titrations of Tel22 (d[A(GGGTTA)$_3$]), a model of the human telomere sequence, using a fluorescent indicator to determine $[K^+]_{free}$ and circular dichroism to assess the extent of folding. At $[K^+]_{free}$ = 5 mM (sufficient for >95% folding), the apparent binding stoichiometry is 3K^+/Tel22; at $[K^+]_{free}$ = 20 mM, it increased to 8–10K^+/Tel22. Thermodynamic analysis shows that at $[K^+]_{free}$ = 5 mM, K^+ binding contributes approximately −4.9 kcal/mol for folding Tel22. The overall folding free energy is −2.4 kcal/mol, indicating that there are energetically unfavorable contributions to folding. Thus, quadruplex folding is driven almost entirely by the energy of cation binding with little or no contribution from other weak molecular interactions.

1. Introduction

Telomeres are nucleic acid–protein complexes that retard erosion of chromosomal ends during DNA replication [1,2]. Human telomeric DNA consists of several kilobases of the repeat sequence 5′-TTAGGG, found mostly in duplex form. However, the 3′ end of the chromosome is unpaired, with a single-stranded overhang whose length varies depending on conditions within the cell that promote or hinder telomere replication during cell division. The nucleotide composition of the telomeric hexanucleotide strongly suggests that it folds in vivo into a series of G-quadruplex structures [3–7]. The basic structural unit of the quadruplex is the G-quartet, a macrocyclic arrangement of four internally H-bonded G residues. Multiple G-quartets stack upon each other, resulting in the formation of four-stranded structures (reviewed in references [8,9]).

Formation of stable quadruplexes can be induced by monovalent cations that coordinate with the guanine O6 atoms that project into the central cavity of the G-quartet (Fig. 1). Because K^+ is the predominant intracellular cation, it is presumed to be the major driving force for formation of G-quadruplexes in vivo [1]. However, other monovalent cations such as Na^+ or NH_4^+ can also promote quadruplex formation in vitro [10]. High-resolution structural studies indicate that K^+ ions are always equidistant between each quartet plane (Fig. 1B), and form the eight oxygen atoms into a symmetric tetragonal bipyramidal configuration [10,11]. In addition to cation binding to the canonical internal binding sites, several quadruplex structures have been shown to bind cations externally, generally to sites formed within the loops connecting adjacent G-quartets [12]. In addition to specific cation binding sites such as those described above that are composed of specific constellations of atoms, it is also well-known that polyanions such as DNA electrostatically attract a sheath of cations that partially neutralizes the backbone phosphates [13,14]. These diffusely bound cations differ structurally and thermodynamically from cations that are bound to specific sites such as the ones discussed above for quadruplexes [15], and their binding depends strongly on the exact shape and phosphate spacing [16].

The 22-mer oligonucleotide d[AGGG(TTAGGG)$_3$] (Tel22), along with similar sequences that contain additional short 5′ and/or 3′ flanking bases have served as models for a single quadruplex within a human telomere (for a review, see reference [17]). Tel22 forms a well-defined structure in the presence of Na^+ in which four segments of DNA are arranged in an antiparallel fashion to form a “basket” topology in which the three TTA sequences form loops connecting the three G-quartets [18]. Each G-quartet contains a Na^+ cation coordinated within its central cavity to give a binding stoichiometry of 3 Na^+/DNA molecule. In contrast, quadruplexes crystallized in the presence of K^+ adopt a different topology in which the strands lie in an all-parallel, propeller-like arrangement with two K^+ ions coordinated between the three G-quartets (Fig. 1B) [19]. However, in K^+ solutions, biophysical studies indicate that the propeller topology is not the predominant structure for Tel22 [20]. The predominant solution states for Tel22 have been suggested to consist of a mixture of structures in which either strand 1 or strand 4 is in a parallel orientation (the so-called hybrid-1 and hybrid-2 arrangements) while the other strands are antiparallel to each other [17,21]. A derivative of Tel22, referred to here as Tel24, which has d[T]$_2$ in place of 5′ dA in Tel22 along with a 3′ dA addition, has been shown by NMR to form predominantly a hybrid-1 type structure in the presence of K^+ [22].

Abbreviations: PBFI, potassium-binding benzofuran-isophthalate; Tel 22, 5′AGGG(TTAGGG)$_3$; Tel 24, 5′ TTGGG(TTAGGG)$_3$A; SVD, singular value decomposition.

* Corresponding author. Tel.: +1 502 852 1172; fax: +1 502 852 1153.
E-mail address: j.chaires@louisville.edu (J.B. Chaires).

0301-4622/$ – see front matter © 2011 Elsevier B.V. All rights reserved.
doi:10.1016/j.bpc.2011.06.012

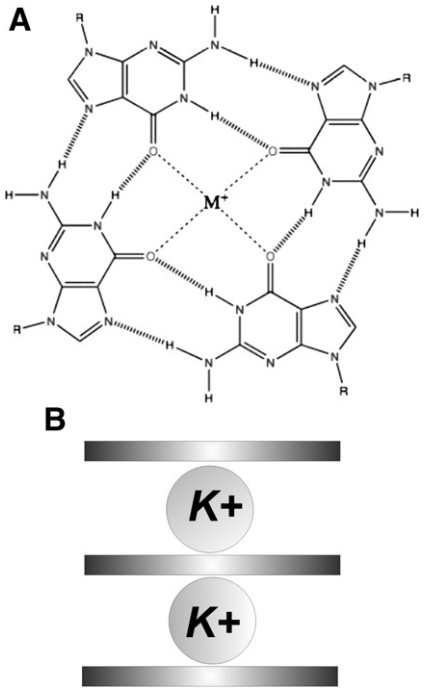

Fig. 1. Panel A shows a G-quartet, the fundamental building block of the G-quadruplex. Four guanine residues are linked in a cyclic arrangement by Hoogstein hydrogen bonds. A monovalent cation M^+ is shown coordinated to the guanine O6 atoms in the central cavity of the quartet. Panel B schematically depicts three stacked G-quartets as found in Tel22. X-ray crystallography indicates that one K^+ ion is coordinated between each pair of quartets to give a K^+ binding stoichiometry of 2 K^+/Tel22.

One aim of the current study was to directly measure quadruplex K^+ binding stoichiometry. The overall cation-dependent quadruplex folding reaction can be represented as $U + \nu K^+ \leftrightarrow F - K^+_\nu$ in which U represents the unfolded ensemble of DNA conformers, F represents the folded quadruplex structures, and the stoichiometric coefficient ν defines the number of cation binding sites in the folded state. Previous titration studies revealed that folding of Tel22 (as assessed by K^+-induced changes in UV absorbance) is cooperative with a Hill coefficients $n = 1.5$ and mid-point $[K^+]$ value of 0.5 mM for Tel22 [23]. Although the Hill coefficient is roughly consistent with $\nu = 2.0$ as expected from structural studies, it nevertheless is an indirect measurement whose meaning is not precisely clear. The uses and misuses of the Hill coefficient as a measure of cooperativity have been thoroughly discussed [24,25].

The impetus for the current direct K^+ binding experiments derives from our observation of a biphasic change in fluorescent emission with respect to [KCl] for derivatives of Tel22 containing serial substitutions of the fluorescent adenine analog, 2-aminopurine [26]. Titrations with NaCl of the same 2-aminopurine-containing oligonucleotides were monophasic, suggesting the possibility that the biphasic K^+ titration profiles reflect the presence of K^+-specific external binding sites. An unrestrained molecular dynamics study of Tel22 in the presence of sufficient K^+ to neutralize the backbone phosphates of Tel22 indicated at least one external site of increased K^+ occupancy in support of the titration data [26]. Thus, the major goal of the current study was to determine directly the value of the binding stoichiometry ν for quadruplex DNA models. To do so, we used the fluorescent indicator PBFI [27,28]. Use of PBFI allows determination of the free K^+ concentration as a function of added KCl in solutions in the absence and presence of an oligonucleotide. This method is analogous to an equilibrium dialysis experiment but is perhaps more accurate and is simpler to carry out [29].

Our experimental strategy exploits the fact that "bulky" cations are unable to form the coordination complexes such as illustrated in Fig. 1 and thus do not drive the folding reaction [10]. In the tetrabutylammonium phosphate buffer system we use, the oligonucleotide strand will remain unfolded until potassium cation is added to drive the folding reaction. We assume that the tetrabutylammonium cation will satisfy the polyelectrolyte need of oligonucleotide to neutralize the backbone phosphates (approximately 0.76 territorially-bound cations per phosphate). Added potassium ions then are expected to bind to the specific sites that are coupled to folding into the quadruplex structure. As a control, we employed a single-stranded oligonucleotide ($d[T]_{22}$) that is expected to be largely unstructured in varying concentrations of KCl.

A second aim of our study was to parse the Gibbs free energy of the overall folding reaction into the contributions of cation binding and oligonucleotide folding. A rigorous, detailed theory for model-independent thermodynamic analysis of Mg^{2+} binding to RNAs that allows estimation of the contribution of Mg^{2+} interactions to folding has been developed by Misra and Draper [15,30,31]. An analogous approach should be applicable to K^+ interaction with quadruplex DNA. We used the thermodynamic theory of Wyman [32] to analyze the K^+ titration data to obtain the overall free energy of K^+-oligonucleotide interaction, along with model-independent folding free energy values determined from titration studies that used circular dichroism to monitor folding. The combined data allowed us to construct a free energy diagram that defines the coupling of K^+ binding to folding. To our surprise, quadruplex folding seems to be driven almost entirely by the free energy of cation binding.

2. Experimental procedures

2.1. Materials

The quadruplex-forming oligonucleotides Tel22, Tel24 and the control oligonucleotide $d[T]_{22}$ were obtained in desalted form from Integrated DNA Technologies, Coralville, IA. The lyophilized oligonucleotides were reconstituted in sufficient buffer (10 mM tetrabutylammonium phosphate, pH 7.0, containing 1 mM EDTA) to give a strand concentration of ~0.5 mM. These solutions were dialyzed for several days against two 500 ml changes of buffer to partially remove a fluorescent impurity. DNA concentrations were estimated from the absorbance at 260 nm using absorptivity values supplied by the manufacturer of 228.5 for Tel22, 244.3 for Tel24, and 178.8 $mM^{-1}\,cm^{-1}$ for $d[T]_{22}$. The K^+ indicator, a tetraammonium salt of PBFI, was from Invitrogen, Carlsbad, CA. A 1 mM stock solution was prepared in water and stored at −20 °C. The PBFI stock concentration was estimated from its absorbance at 345 nm using $\varepsilon = 42\ mM^{-1}\,cm^{-1}$ [33].

2.2. Determination of $[K+]_{free}$

PBFI, a fluorescent K^+ indicator, was used to compare $[K^+]_{free}$ in the oligonucleotide solution of interest to that in buffer lacking the oligonucleotide. PBFI is a benzofuran-isophthalate crown ether that has been used to measure $[K^+]_{free}$ by measuring changes in fluorescence emission of the indicator molecule with added K^+ [27]. Fluorescence titrations were conducted in a micro-fluorescence cuvette of ~150 μL volume using a FluoroMax-3 instrument (HORIBA Jobin Yvon Inc., Edison, NJ). The temperature of the cuvette was maintained at 25 °C with a circulating water bath. Excitation was at 350 nm (2 nm bandwidth). Emission spectra for buffer, DNA in buffer, and after each addition of KCl were recorded over the wavelength range 400–600 nm (5 nm bandwidth). The individual emission spectra were corrected by subtracting a blank spectrum of either reference buffer or oligonucleotide solution as appropriate. Emission spectra for buffer titrations were also corrected for dilution by the

added KCl (maximum of ~20%); however, control titrations of the oligonucleotide solutions with KCl showed that a compensating small increase in apparent emission intensity at 472 nm with increasing [KCl] made correction for dilution unnecessary.

2.3. CD titration studies

Titration studies of cation-dependent folding of the telomeric oligonucleotides into quadruplex structures were monitored by circular dichroism as previously described [26].

3. Results

3.1. Determination of K^+:oligonucleotide binding stoichiometry

Fig. 2A shows the cation binding stoichiometry for Tel22 and dT22 as calculated from fluorometric titrations using the BPFI indicator to measure $[K^+]_{free}$. Tel22 clearly binds more K^+ than $d[T]_{22}$ at values of $[K^+]_{free}$ between ~0.5 and 14 mM KCl. At $[K^+]_{free}$ of 2.5 mM, ~2 K^+ are bound per Tel22 DNA molecule; at higher $[K^+]_{free}$, the apparent binding increases to ~3 K^+/DNA molecule at 5 mM KCl and approaches ~8 K^+/molecule at 12 mM KCl. For Tel24, a sequence that folds exclusively into a hybrid 1 conformation, binding stoichiometries of 2–4 K^+/DNA were observed over the same concentration range (see Supplementary Material).

The total work of ligation can be estimated from the data of Fig. 2A using concepts developed by Wyman [32]. The free energy of ligation can be estimated for any extent of the reaction using the integral

$$\Delta G = RT\int_0^X \ln x d\overline{X} \quad (1)$$

where $\overline{X}$ is the average number of bound K^+/DNA at $[K^+]_{free} = x$ [32]. Integration of each of the data sets in Fig. 2A results in the data plotted in Fig. 2B. This figure shows the total free energy of ligation at 25 °C up to ~12 mM $[KCl]_{free}$. These values reflect the contributions of specific, non-specific, diffuse K^+ binding and conformational changes such as folding. Inspection of Fig. 2B shows that at 25 °C, 5 mM KCl, conditions where Tel22 is fully folded into quadruplex structures, ΔG values of −2.1 and −0.2 kcal/mol for Tel22 and $d[T]_{22}$ are observed.

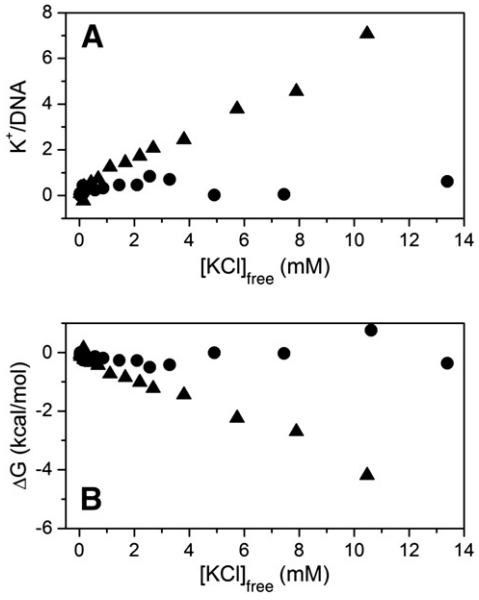

Fig. 2. Panel A: Plot of the average number of bound K^+ cations per DNA molecule as a function of $[KCl]_{free}$ for Tel22 (▲) and $d[T]_{22}$ (●) as determined by titrations with KCl in the presence of the fluorescent K^+ indicator, PBFI. Panel B: total free energy of ligation at 25 °C up to ~12 mM $[KCl]_{free}$ for Tel22 (▲) and $d[T]_{22}$ (●) calculated from Eq. (1).

3.2. Quadruplex folding assessed by circular dichroism titration

Fig. 3A shows K^+-driven folding of Tel22 into quadruplex structures as monitored by circular dichroism at 295 nm, a wavelength sensitive to G-quartet stacking [34]. Complete spectra and data analysis are shown in Supplementary Materials. The titration curve is complete with clear pre- and post-transition baselines. The transition midpoint is near 0.3 mM KCl, and the span of the titration curve (from 10 to 90% completion) is approximately 1 mM KCl.

The titration data shown in Fig. 3A were analyzed to obtain apparent equilibrium constants as a function of total KCl concentration. SVD analysis of complete spectra collected as a function of KCl concentration (shown in Supplementary Material) revealed two prominent singular values that together account for 99.87% of the variance observed in the family of the spectra, indicating that a simple two-state analysis of the titration data is justified. The presence of a minor third species is suggested from the autocorrelation analysis of SVD basis spectra and amplitude vectors, but its contributions to the amplitude of the spectral changes over the titration are negligible, accounting for only 0.13% of the total variance. For an apparent two-state process, the equilibrium constant at each KCl concentration is

$$K_{app} = \frac{\theta - \theta_i}{\theta_f - \theta_i} \quad (2)$$

where θ is the observed ellipticity, θ_i is the ellipticity in the absence of KCl, and θ_f is the ellipticity of the fully folded form. Data over the range of 10 to 90% folded were used to calculate equilibrium constants [35]. The titration in Fig. 3A yields the linear relation

$$\ln K_{app} = (12.94 \pm 0.18) + (1.56 \pm 0.02)\ \ln[KCl] \quad (3)$$

with a correlation coefficient of 0.998. The standard deviations of the fitted parameters are indicated. Calculated apparent folding free energies, $\Delta G_{app} = -RT \ln K_{app}$, are shown in Fig. 3B.

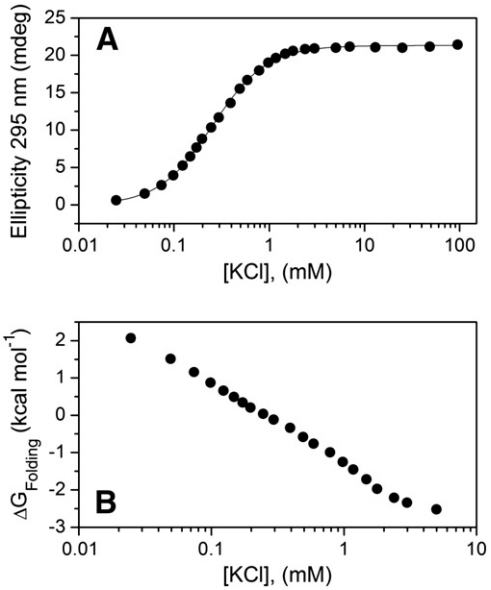

Fig. 3. Panel A: Folding of Tel 22 assessed by changes in ellipticity at 295 nm. Panel B: $\Delta G_{folding}$ of Tel22 as a function of [KCl] calculated from Eq. (1).

4. Discussion

Cations play a crucial role in G-quadruplex folding [10,36] and dictate the conformation of the folded form for the human telomeric quadruplex [7,9,37–39]. The experiments described here provide a detailed understanding of potassium-driven folding of human telomeric DNA sequences. First, our results show that the folded telomeric DNA sequences in this study bind more than the two K^+ ions predicted solely from the two coordination sites located between the G stacks (Fig. 1A). Second, we provide evidence that the number of bound K^+ depends on the folding topology of the quadruplex, since Tel22 binds more of the cation at a given free cation concentration than Tel24 (Fig. S1A). Finally, through linkage analysis, we define the contribution of potassium binding to the thermodynamic stability of the folded quadruplex. We discuss these findings below.

Our determination of the stoichiometry of K^+ binding clearly shows that at >2.5 mM KCl, Tel22 binds up to 6–8 more K^+ than the two ions predicted from the crystallographic analysis which shows K^+ located between the three quadruplex stacks. Tel24 also binds 1–2 additional K^+ in excess of the two centrally-bound ions in the concentration range up to ~20 mM KCl. It is important to note that the indicator titrations do not distinguish between specifically bound cations and non-specifically (diffusely) bound cations because both modes of interaction will result in a decrease in the cation activity sensed by the indicator. Indeed, the data of Fig. S1 indicates increasing apparent K^+ binding to Tel22 up to the sensitivity limits of the titration (~20–25 mM KCl). A portion of this binding at higher [KCl] may represent diffusely bound cations. The differences between these two classes are: (a) specifically bound cations bind stoichiometrically to defined electronegative sites on the polyelectrolyte; (b) specific complexes do not retain inner sphere water molecules; and (c) specific binding processes follow mass action [15]. In contrast, diffusely bound cations are attracted to the high negative charge density of the phosphate backbone, thereby stabilizing it by reducing the electrostatic repulsion due to the closely spaced phosphate groups. Diffusely bound cations tend to retain inner sphere water molecules. Thus, by reducing electrostatic repulsion, diffuse cations promote polyelectrolyte folding without binding to specific sites.

The number of condensed cations varies with the shape of the polyelectrolyte. Manning theory predicts approximately 0.88 monovalent cations per phosphate group for an infinitely long cylinder such as a DNA double helix, but the level of condensed cation binding to quadruplexes has not been determined. The number might be expected to be larger as a result of the more compact structure of the folded quadruplex molecule. Comparison of the results obtained for the quadruplexes with those of unstructured $d[T]_{22}$ suggest 1–2 diffusely bound potassium cations per quadruplex under our experimental conditions (e.g. 10 mM butyl ammonium phosphate, with approximately 50% of the butyl ammonium ions in the cationic state). If this is the case, then Tel22 may specifically bind up to 5 cations to external sites, while Tel24 may bind ~1 cation to an external site.

Previous studies with rare earth ions also show that quadruplexes bind these cations to external sites. Based on changes in Tb^{3+} luminescence Galezowska et al. [40] reported that a 21-mer oligonucleotide identical to Tel22 but lacking the 5′-dA residue binds 5–7 Tb^{3+} per quadruplex molecule. These authors provided CD and luminescence data suggesting that two Tb^{3+} bind to quadruplex internal sites and the remaining 3–5 Tb^{3+} bind to external (loop) sites. The luminescence studies are reminiscent of our KCl titrations of 2-aminopurine derivatives of Tel22 monitored by changes in fluorescence [26]. In these studies, we observed a biphasic response to added KCl similar to that observed for the Tb^{3+} titrations. For our KCl titrations of 2-aminopurine/Tel22 oligonucleotides, the maximum in emission intensity occurred at 2–3 mM K^+ and subsequently decreased over a range of 20 to 100 mM KCl. Titrations of the same oligonucleotide with NaCl were monophasic [26], thus showing that the effect was specific for K^+ and not a general ionic effect on 2-aminopurine fluorescence.

Despite the crucial role of cations in quadruplex folding, the thermodynamic linkage between cation binding and folding had yet to be fully described prior to this work. The data presented here allows this linkage to be quantified. At 5 mM KCl, the Tel 22 quadruplex is fully folded. From Figs. 2B and 3B, the free energy of folding at 5 mM KCl is estimated to be −2.1 and −2.7 kcal/mol from ion binding experiments and CD measurements, respectively. These values are in good agreement and average to a value of −2.4 kcal/mol for the overall folding reaction. From the slope $\partial \ln K_{app}/\partial \ln[KCl]$determined from the data in Fig. 3, the free energy contribution from cation association can be estimated as

$$\Delta G_{ion} = \left[\frac{\partial \ln K}{\partial \ln[KCl]}\right] RT \ln[KCl] \quad (5)$$

At 5 mM KCl, ΔG_{ion} is −4.9 kcal/mol. The coupling free energy is the difference between the observed folding free energy and ΔG_{ion}, a value of about +2.5 kcal/mol. Fig. 4 summarizes these relationships. The free energy diagram indicates that the overall folding process must contain a "hidden" contribution that is energetically unfavorable. We speculate that the unfavorable free energy arises from an unligated folded species. A surprising consequence of the scheme in Fig. 4 is the conclusion that quadruplex folding is driven almost entirely by the energy of cation binding, with little or no contribution from other weak molecular interactions within the G-quartet stack.

The insignificant energetic contribution of molecular interactions within the G-quartet stack to folding, while surprising, is supported by a recent computational study [41]. In that study, solvent and salt effects on the structural stability of human telomere quadruplex conformers were studied using three-dimensional reference interaction site model theory [42]. The results showed that in pure water the "conformation energy" was positive and unfavorable for all quadruplex conformers examined, but that large, favorable solvation free energies overwhelmed that unfavorable energy to yield stable conformers. The computed "conformation energy" contains contributions from bonding, bending, torsion

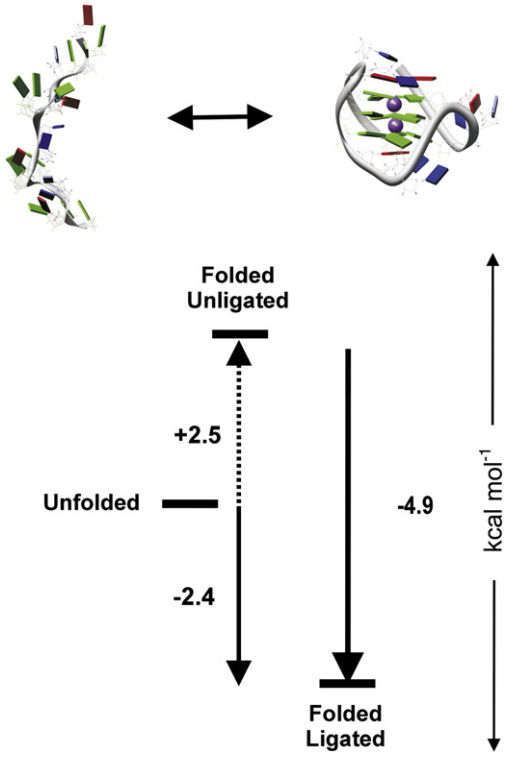

Fig. 4. Free energy diagram summarizing the energetics of K^+-driven folding of Tel22.

energy, Lennard–Jones and electrostatic terms, and thus would reflect the balance of molecular interactions in the structure in the absence of solvent molecules. The computed unfavorable "conformation energy" is qualitatively consistent with the positive free energy we infer that is associated with a folded but unligated structure (Fig. 4).

Acknowledgments

Supported by grants GM077422 and CA35635 from the National Institutes of Health, by NIH/NCRR COBRE P20RR018733 and by the James Graham Brown Foundation.

Appendix A. Supplementary data

Supplementary data to this article can be found online at doi:10.1016/j.bpc.2011.06.012.

References

[1] J.R. Williamson, M.K. Raghuraman, T.R. Cech, Monovalent cation-induced structure of telomeric DNA: the G-quartet model, Cell 59 (1989) 871–880.
[2] J.L. Osterhage, K.L. Friedman, Chromosome end maintenance by telomerase, J. Biol. Chem. 284 (2009) 16061–16065.
[3] L.H. Hurley, DNA and its associated processes as targets for cancer therapy, Nat. Rev. Cancer 2 (2002) 188–200.
[4] H.J. Lipps, D. Rhodes, G-quadruplex structures: in vivo evidence and function, Trends Cell Biol. 19 (2009) 414–422.
[5] N. Maizels, Dynamic roles for G4 DNA in the biology of eukaryotic cells, Nat. Struct. Mol. Biol. 13 (2006) 1055–1059.
[6] S. Neidle, G. Parkinson, Telomere maintenance as a target for anticancer drug discovery, Nat. Rev. Drug Discov. 1 (2002) 383–393.
[7] S. Neidle, G.N. Parkinson, The structure of telomeric DNA, Curr. Opin. Struct. Biol. 13 (2003) 275–283.
[8] M.A. Keniry, Quadruplex structures in nucleic acids, Biopolymers 56 (2001) 123–146.
[9] A.N. Lane, J.B. Chaires, R.D. Gray, J.O. Trent, Stability and kinetics of G-quadruplex structures, Nucleic Acids Res. 36 (2008) 5482–5515.
[10] N.V. Hud, J. Plavec, The role of cations in determining quadruplex structure and stability, in: S. Balasubramanian, S. Neidle (Eds.), Quadruplex Nucleic Acids, RSC Publishing, Cambridge, UK, 2006, pp. 100–130.
[11] S. Burge, G.N. Parkinson, P. Hazel, A.K. Todd, S. Neidle, Quadruplex DNA: sequence, topology and structure, Nucleic Acids Res. 34 (2006) 5402–5415.
[12] R. Ida, G. Wu, Direct NMR detection of alkali metal ions bound to G-quadruplex DNA, J. Am. Chem. Soc. 130 (2008) 3590–3602.
[13] G.S. Manning, The molecular theory of polyelectrolyte solutions with applications to the electrostatic properties of polynucleotides, Q. Rev. Biophys. 11 (1978) 179–246.
[14] M.T. Record Jr., C.F. Anderson, T.M. Lohman, Thermodynamic analysis of ion effects on the binding and conformational equilibria of proteins and nucleic acids: the roles of ion association or release, screening, and ion effects on water activity, Q. Rev. Biophys. 11 (1978) 103–178.
[15] V.K. Misra, D.E. Draper, On the role of magnesium ions in RNA stability, Biopolymers 48 (1998) 113–135.
[16] G. Lamm, G.R. Pack, Counterion condensation and shape within Poisson–Boltzmann theory, Biopolymers 93 (2010) 619–639.
[17] J. Dai, M. Carver, D. Yang, Polymorphism of human telomeric quadruplex structures, Biochimie 8 (2008) 1172–1183.
[18] Y. Wang, D.J. Patel, Solution structure of the human telomeric repeat d[$AG_3(T_2AG_3)_3$] G-tetraplex, Structure 1 (1993) 263–282.
[19] G.N. Parkinson, M.P. Lee, S. Neidle, Crystal structure of parallel quadruplexes from human telomeric DNA, Nature 417 (2002) 876–880.
[20] J. Li, J.J. Correia, L. Wang, J.O. Trent, J.B. Chaires, Not so crystal clear: the structure of the human telomere G-quadruplex in solution differs from that present in a crystal, Nucleic Acids Res. 33 (2005) 4649–4659.
[21] J. Dai, M. Carver, C. Punchihewa, R.A. Jones, D. Yang, Structure of the Hybrid-2 type intramolecular human telomeric G-quadruplex in K^+ solution: insights into structure polymorphism of the human telomeric sequence, Nucleic Acids Res. 35 (2007) 4927–4940.
[22] K.N. Luu, A.T. Phan, V. Kuryavyi, L. Lacroix, D.J. Patel, Structure of the human telomere in K^+ solution: an intramolecular (3 + 1) G-quadruplex scaffold, J. Am. Chem. Soc. 128 (2006) 9963–9970.
[23] R.D. Gray, J.B. Chaires, Kinetics and mechanism of K^+- and Na^+-induced folding of models of human telomeric DNA into G-quadruplex structures, Nucleic Acids Res. 36 (2008) 4191–4203.
[24] J.M. Holt, G.K. Ackers, The Hill coefficient: inadequate resolution of cooperativity in human hemoglobin, Methods Enzymol. 455 (2009) 193–212.
[25] J.N. Weiss, The Hill equation revisited: uses and misuses, FASEB J. 11 (1997) 835–841.
[26] R.D. Gray, L. Petraccone, J.O. Trent, J.B. Chaires, Characterization of a K^+-induced conformational switch in a human telomeric DNA oligonucleotide using 2-aminopurine fluorescence, Biochemistry 49 (2010) 179–194.
[27] A. Minta, R.Y. Tsien, Fluorescent indicators for cytosolic sodium, J. Biol. Chem. 264 (1989) 19449–19457.
[28] K. Meuwis, N. Boens, F.C. De Schryver, J. Gallay, M. Vincent, Photophysics of the fluorescent K^+ indicator PBFI, Biophys. J. 68 (1995) 2469–2473.
[29] D. Grilley, A.M. Soto, D.E. Draper, Direct quantitation of Mg^{2+}-RNA interactions by use of a fluorescent dye, Methods Enzymol. 455 (2009) 71–94.
[30] V.K. Misra, D.E. Draper, A thermodynamic framework for Mg^{2+} binding to RNA, Proc. Natl. Acad. Sci. USA 98 (2001) 12456–12461.
[31] V.K. Misra, R. Shiman, D.E. Draper, A thermodynamic framework for the magnesium-dependent folding of RNA, Biopolymers 69 (2003) 118–136.
[32] J. Wyman, S.J. Gill, Binding and Linkage: Functional Chemistry of Biological Molecules, University Science Books, Mill Valley, CA, 1990.
[33] Molecular Probes Handbook, Invitrogen, Carlsbad, CA, 2003.
[34] J.L. Mergny, A.T. Phan, L. Lacroix, Following G-quartet formation by UV-spectroscopy, FEBS Lett. 435 (1998) 74–78.
[35] D.A. Deranleau, Theory of the measurement of weak molecular complexes. I. General considerations, J. Am. Chem. Soc. 91 (1969) 4044–4049.
[36] A.E. Engelhart, J. Plavec, O. Persil, N.V. Hud, Metal ion interactions with G-quadruplex structures, in: N.V. Hud (Ed.), Nucleic Acid–Metal Ion Interactions, Royal Society of Chemistry, Cambridge, 2008, pp. 114–149.
[37] S. Neidle, The structures of quadruplex nucleic acids and their drug complexes, Curr. Op. in Struct. Biol. 19 (2011) 239–250.
[38] D.J. Patel, A.T. Phan, V. Kuryavyi, Human telomere, oncogenic promoter and 5′-UTR G-quadruplexes: diverse higher order DNA and RNA targets for cancer therapeutics, Nucleic Acids Res. 35 (2007) 7429–7455.
[39] D. Yang, K. Okamoto, Structural insights into G-quadruplexes: towards new anticancer drugs, Future Med. Chem. 2 (2010) 619–646.
[40] E. Galezowska, A. Gluszynska, B. Juskowiak, Luminescence study of G-quadruplex formation in the presence of Tb^{3+} ion, J. Inorg. Biochem. 101 (2007) 678–685.
[41] Y. Maruyama, T. Matsushita, R. Ueoka, F. Hirata, Solvent and salt effects on structural stability of human telomere, J. Phys. Chem. B 115 (2011) 2408–2416.
[42] F. Hirata, Molecular Theory of Solvation, Kluwer Dordrecht, The Netherlands, 2003.